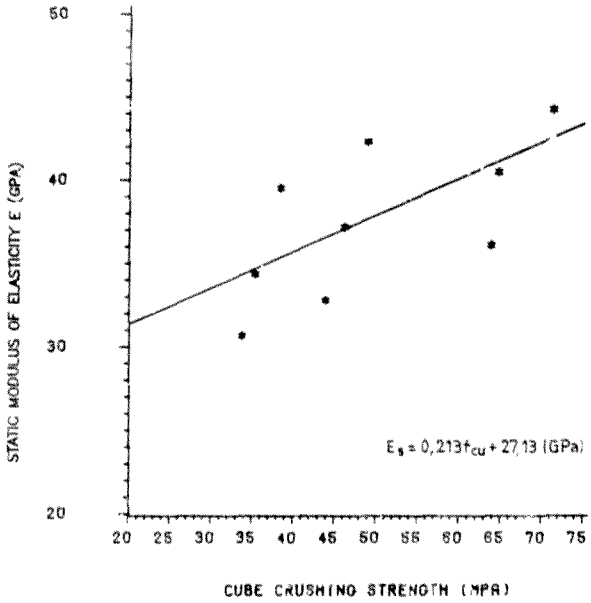

FIG 3.11b CUBE STRENGTH VS. STATIC MODULUS
(ANDESITE CONCRETE)

Both equations are in agreement with equation 3.8. The C_o factor which is closely related to the modulus of elasticity of the aggregate is higher for andesite concrete than for granite concrete. This was expected as the andesite aggregate has a greater elastic modulus than its granite counterpart.

The increase in concrete strength with the increase in modulus of elasticity of the aggregate can be attributed to the effect of aggregate rigidity on stress distribution in the concrete during external loading. If we assume equal strains, the portion of the load which is taken by the aggregate increases with its rigidity and consequently that taken by the paste decreases. The strength of ordinary concrete is determined mainly by the strength of the paste, so a decrease in loading on the paste delays fracture and thereby increases concrete strength. It should be noted that a higher modulus of elasticity usually involves a stronger aggregate[39].

The graph of stone content against static elastic moduli is shown in figure 3.12(a) for granite and andesite concrete. (The curve for c/w = 1.8 for granite is drawn for only two laboratory results as the measurement for c/w = 1.8 at stone content 700 kg/m^3 is inconsistent). The curves show clearly that increasing stone content has a minor effect for granite but an appreciable effect for andesite. Obviously the lower granite aggregate modulus has a lesser effect on the composite concrete modulus than the corresponding effect of the higher andesite aggregate modulus. In the limit when the elastic modulus of the aggregate is equal to the elastic modulus of the mortar, the elastic modulus of the concrete will be independent of volume of aggregate (assuming proper bonding etc.)

However, the c/w ratio has a marked effect on both aggregate types especially the granite concrete. Again increase in c/w ratio and hence increase in the elastic modulus of the mortar

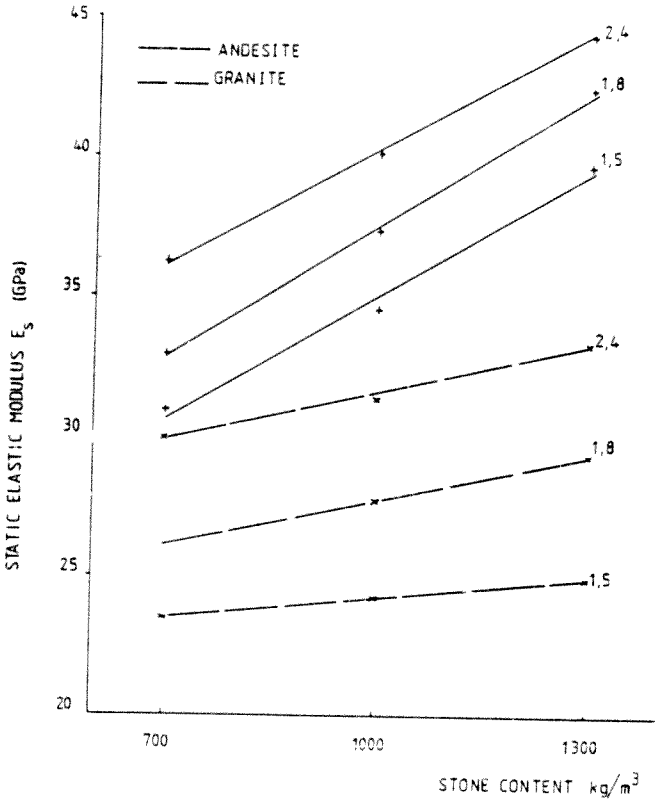

FIG 3.12a STATIC MODULUS Vs. STONE CONTENT SHOWING AFFECT OF INCREASING C/W RATIO FOR GRANITE AND ANDESITE CONCRETE.

would have a more marked effect on the lower modulus granite concrete than the andesite concrete. For both aggregate types the high stone content mixes fit in with the general trend of lower stone content mixes. This shows that the aggregate interparticle contacts occurring in the higher stone content mixes do not appear to have adversely affected the static elastic modulus of the concrete. The concrete failure loads for each mix were fairly consistent indicating good experimental technique. The failure types are shown in figure 2.1(a) of chapter 2 and failed concrete specimens are shown in figure 3.12(b).

Failure type A shows an inclined failure plane, and B is a tensile-type failure due to vertical splitting. Failure type C is an hour glass type failure, where ultimate failure was by crushing. No real pattern of failure for the various stone contents and cement/water ratios was observed. However, failure type B was predominantly the failure pattern for both granites and andesites. Failure type A seldom occurred. Several specimens for both aggregate types failed due to a combination of the failure types shown.

As expected the andesite mixes gave higher elastic modulus values than their granite counterparts. Values for the granite concretes ranged from an average of 23,46 to 33,24 GPa compared to 30,81 to 44,35 GPa for andesite. The tables 3.9(a) and (b) also show the average Poisson's ratio values for the concretes. The Poisson's ratio, ν, is also comparatively constant for both sets of concrete. On average for granite concrete $\nu = 0,18$ and for andesite concrete $\nu = 0,21$.

3.9.1.1 Static Stress/Strain Plots

Stress/strain plots were produced autographically for the specimens on the X-Y plotter. In general the first three plots up to the 'E' load for granite mixes tended to be concave upwards compared with the andesites which tended to be concave downwards. The andesite concretes produced a more linear stress/strain curve than the granites, probably due to the higher

would have a more marked effect on the lower modulus granite concrete than the andesite concrete. For both aggregate types the high stone content mixes fit in with the general trend of lower stone content mixes. This shows that the aggregate interparticle contacts occurring in the higher stone content mixes do not appear to have adversely affected the static elastic modulus of the concrete. The concrete failure loads for each mix were fairly consistent indicating good experimental technique. The failure types are shown in figure 2.17(a) of chapter 2 and failed concrete specimens are shown in figure 3.12(b).

Failure type A shows an inclined failure plane, and B is a tensile-type failure due to vertical [illegible]g. Failure type C is an hour glass type failure, where [illegible]ailure was by crushing. No real pattern of failure [illegible] various stone contents and cement/water ratios was observed. However, failure type B was predominantly the failure pattern for both granites and andesites. Failure type A seldom occurred. Several specimens for both aggregate types failed due to a combination of the failure types shown.

As expected the andesite mixes gave higher elastic modulus values than their granite counterparts. Values for the granite concretes ranged from an average of 23,46 to 33,24 GPa compared to 30,81 to 44,35 GPa for andesite. The tables 3.9(a) and (b) also show the average Poisson's ratio values for the concretes. The Poisson's ratio, ν, is also comparatively constant for both sets of concrete. On average for granite concrete $\nu = 0,18$ and for andesite concrete $\nu = 0,21$.

3.9.1.1 Static Stress/Strain Plots

Stress/strain plots were produced autographically for the specimens on the X-Y plotter. In general the first three plots up to the 'E' load for granite mixes tended to be concave upwards compared with the andesites which tended to be concave downwards. The andesite concretes produced a more linear stress/strain curve than the granites, probably due to the higher

Figure 3.12(b) Typical Failures for Concrete Specimens

aggregate stiffness. However, although the specimens were only cycled up to one third of the ultimate cube strength and in a short-term loading condition, the plots were all somewhat curvi-linear. The curvi-linearity may be due to the differential response of the paste and aggregate as a result of the composite action of the concrete and the cement-aggregate bond. A reduction in bond strength leads to an increase in non-linearity[40]. Hysteresis effects were also evident for both concrete types. However, the granites exhibited greater hysteresis indicated by the area enclosed by the loading and unloading curves which is a measure of the energy dissipated in the specimen. Hysteresis effects reduced from initial plots (plot 1) to final 'E' plots (plot 3).

The complete stress-strain curves to failure showed that when the initial curvi-linear ascending branch exceeded 30% of the ultimate stress level significant external bond cracks were visually observed. Upon increasing to the peak or failure stress, matrix and external bond cracks propagated and finally the curve exhibited a descending branch. The andesite mixes yielded more extensive descending branches and the granite exhibited more rounded curves. The descending branch indicated a capacity of carrying reduced stress at higher strain levels. However, as discussed in chapter 2, the envelope curve is not independent of the load regime e.g. type of testing machine.

The concrete plots were more curvi-linear than the paste or mortar curves shown in chapter 2. This is due to its greater inelasticity. There was no real trend within the three stone contents with respect to the plots. Representative plots for granites and andesites are shown in figures 3.13 and 3.14 respectively. The plots are produced in a form somewhat different from normal stress/strain plots since they were derived directly from the X-Y plotter records. The lateral strain curve is not to the same scale as the longitudinal strain curves. The lateral strain curve stress/strain axis are also omitted for clarity.

Figures 3.13(a) and (b) show the plots for a granite concrete of 1300 kg/m^3 stone content and a cement/water ratio of 1,5. Plot 1 in figure 3.13(a) clearly has greater hysteresis effects than the two successive curves. This 'bedding in' cycle causes damage and hence the energy dissipated is more extensive than following cycles. The stress/strain curve actually changes from a slight concave downwards in plot 1 to approximately linear in plot 2 to concave upwards in plot 3. Plot 3 suggests a strengthening of the material and a greater resistance to deformation. The complete stress/strain curve in figure 3.13(b) is also typical of the granites, the descending branch showing progressive deterioration of the concrete by extensive cracking. It is interesting to note that the longitudinal stress/strain curve and the lateral stress/strain curve follow the same form.

The equivalent andesite concrete is shown in figure 3.14(a) and (b). The plots are more linear and exhibit reduced hysteresis effects compared with the granite concrete. The plots change from concave downward to virtually linear from plot 1 to plot 3. Figure 3.14(b) shows the stress/strain envelope for andesites. In this particular case, the andesite elastic modulus is approximately 61% greater than the granite modulus and the failure load is 15% greater. The curves also show that the limit of the andesite strain in figure 3.14(b) is approximately 3000.10^{-6} while for granite in figure 3.13(b) it is approximately 6000.10^{-6}. This could be attributed to the greater stiffness and angularity of the andesite aggregate mixes i.e. greater deformation resistance under load.

Several of the granite mixes rendered fairly linear stress-strain plots. Figures 3.15(a) and (b) show the plots for a granite concrete having a stone content of 700 kg/m^3 and cement/water ratio of 1,8. Hysteresis and creep effects are evident. The plots show that creep is more extensive in the longitudinal direction (the direction of applied load) than the lateral

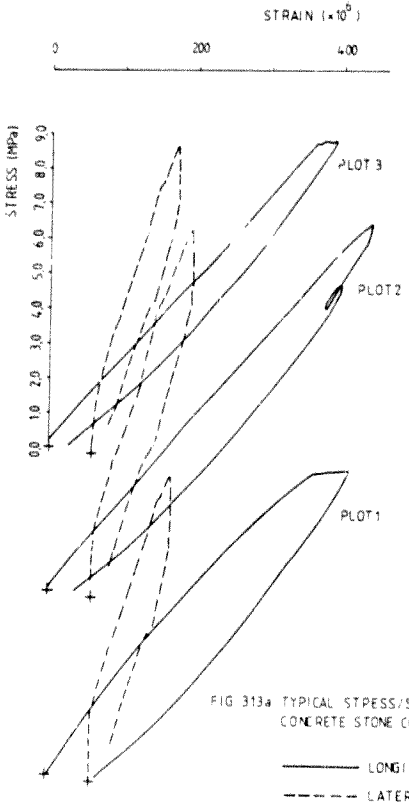

FIG 313a TYPICAL STRESS/STRAIN PLOT FOR GRANITE CONCRETE STONE CONTENT 1300 kg/m^3 c/w = 1.5

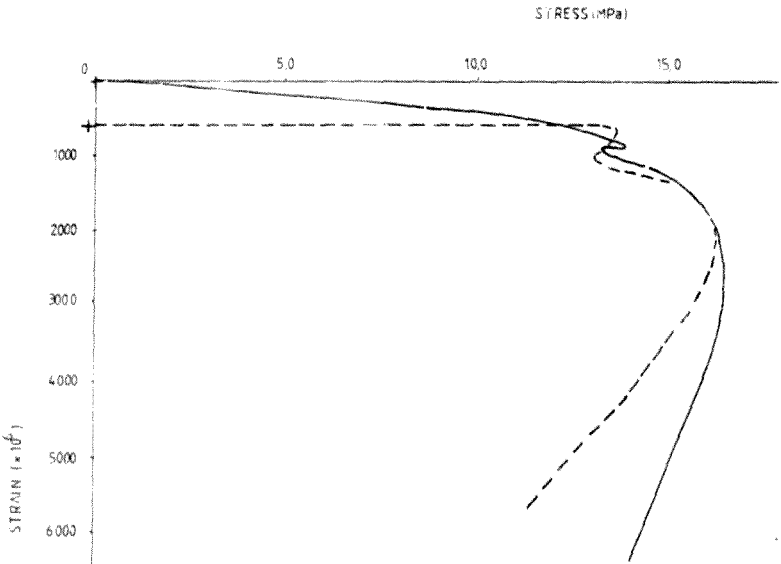

FIG 3.13b STRESS/STRAIN PLOT TO FAILURE FOR GRANITE CONCRETE STONE CONTENT 1300 kg/m³, c/w = 1,5

——— LONGITUDINAL STRAIN

– – – – LATERAL STRAIN

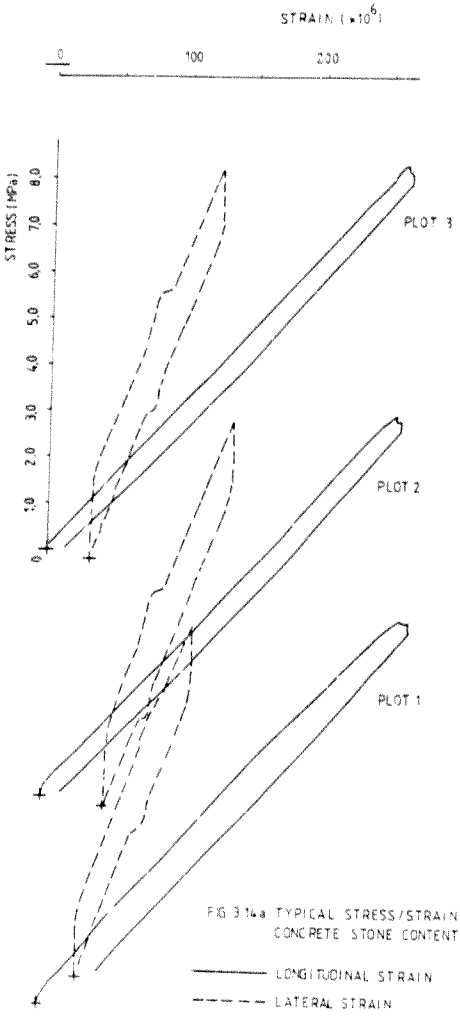

FIG 3.14a TYPICAL STRESS/STRAIN PLOT FOR ANDESITE CONCRETE STONE CONTENT 1300 kg/m^3 c/w = 1.5

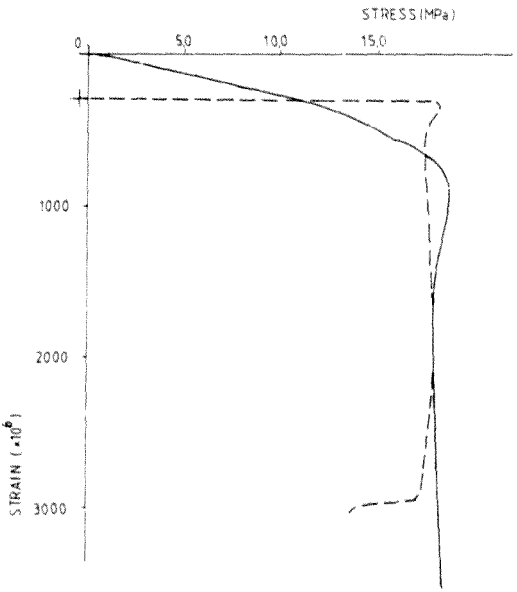

FIG 3.14b TYPICAL STRESS/STRAIN PLOT TO FAILURE FOR ANDESITE CONCRETE STONE CONCRETE 1300 k, m^3 c/w=1,5

——— LONGITUDINAL STRAIN

– · – · – · LATERAL STRAIN

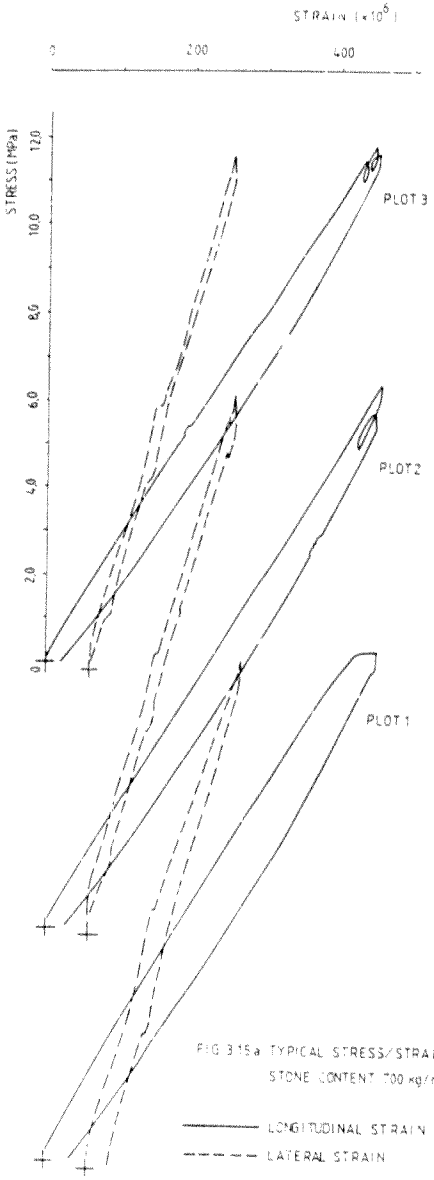

FIG 3.15a TYPICAL STRESS/STRAIN PLOTS FOR GRANITE CONCRETE
STONE CONTENT 700 kg/m^3 c/w = 1.8

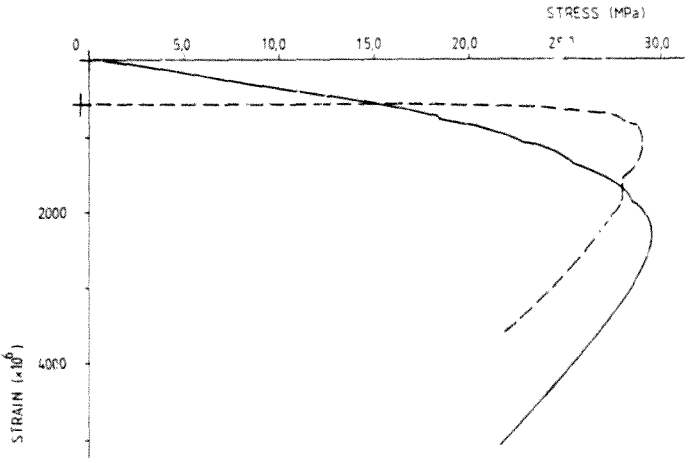

FIG 3.15b STRESS/STRAIN PLOT TO FAILURE FOR GRANITE CONCRETE
STONE CONTENT 700 kg/m^3, c/w = 1,8

——— LONGITUDINAL STRAIN
– – – – LATERAL STRAIN

direction. In general, the granites displayed greater creep movement than the andesites.

The corresponding andesite mix is plotted in figure 3.16 and displays more uniform stress/strain curves than the granites and again reduced hysteresis. These plots are concave downwards to linear. Although both mixes have comparable prism strengths, (granite failure load 316,8 kN and andesite 313,2 kN), the andesite mix has a static modulus of 34,7 GPa compared to the granite modulus of 26,63 GPa. Thus the static modulus of the andesite is 30% greater than that of the granite mix. This result shows the importance of the aggregate stiffness with respect to the composite concrete stiffness - all other factors being equal. The greater the aggregate stiffness, the higher the modulus of the concrete.

3.9.2 Comparison of Elastic Moduli for Concrete

The results of the electrodynamic and ultrasonic tests are given in appendixes E and F respectively. Tables 3.10(a) and (b) give the average values for the above moduli. From both tables there would appear to be major inconsistencies with respect to the electrodynamic elastic modulus values. This could possibly be due to some inaccuracies or oversights in the experimental method. Sometimes the fundamental frequency was not so clearly defined. Since the square of the fundamental frequency is proportional to the dynamic modulus, substantial errors can occur.

The ultrasonic modulus is considerably greater than the electrodynamic modulus in general. A typical plot is shown in figure 3.17. The curves show c/w ratio against static, electrodynamic and ultrasonic moduli for an andesite concrete, stone content 1300 kg/m^3. The plots show that the ultrasonic modulus is approximately twice that of the static and electrodynamic. However, the ultrasonic test is sensitive to

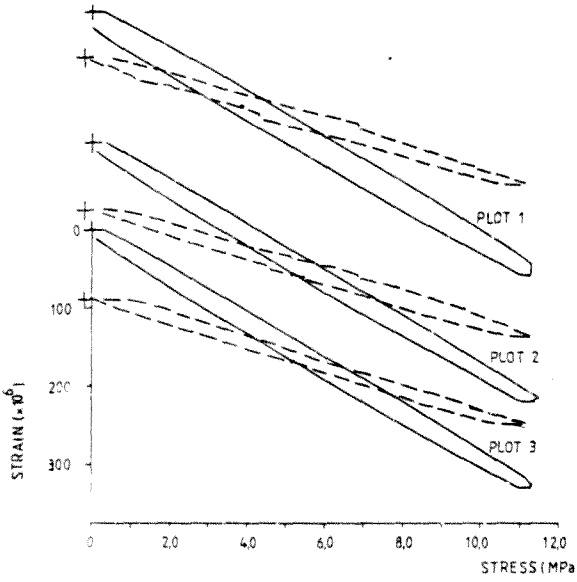

FIG 3.16a TYPICAL STRESS/STRAIN PLOTS FOR ANDESITE CONCRETE. STONE CONTENT 700 kg/m^3, c/w = 1,8

——— LONGITUDINAL STRAIN

– – – – LATERAL STRAIN

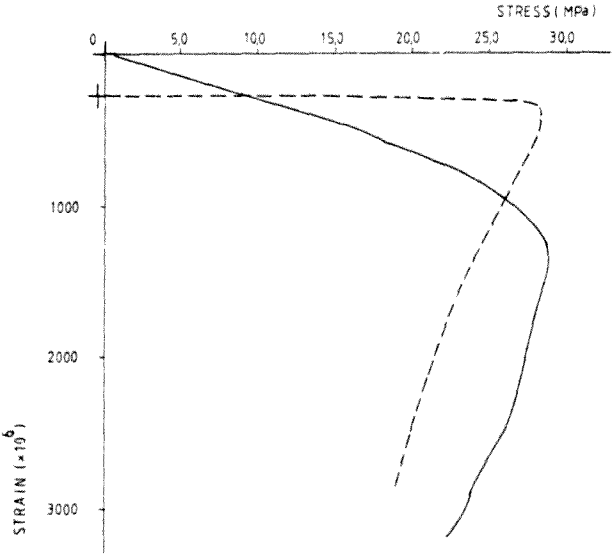

FIG 3.16b STRESS/STRAIN PLOT TO FAILURE FOR ANDESITE CONCRETE
STONE CONTENT 700 kg/m^3 c/w = 1.8

variations in moisture content[41]. The pulse velocity increases with increasing moisture content. Therefore variations in moisture content would affect the pulse velocity which would affect the ultrasonic modulus considerably.

Comparing table 3.9 and 3.10 it is evident that the electrodynamic modulus is approximately equal to the static modulus. Figure 3.17 shows that for the case quoted the static modulus is slightly greater than the electrodynamic modulus. However, in some other cases the electrodynamic modulus was about 30 percent greater than the corresponding static modulus. This is true for both granite and andesite mixes. It would appear that the accuracy of the electrodynamic tests performed for this work is not very good.

Table 3.10(a) and (b) also shows that the electrodynamic and ultrasonic dynamic moduli increase with increasing stone content. This has a slight effect on the electrodynamic moduli, but a more pronounced effect on the ultrasonic moduli. As is the case with static modulus, the andesites exhibit higher electrodynamic and ultrasonic moduli than the granites. Figure 3.18 and 3.19 show plots of static elastic modulus against electrodynamic and ultrasonic moduli for granite and andesite concrete respectively. A linear regression line is fitted for each set of data. Figure 3.18 for granite concrete shows a greater scatter of results compared to the andesite results shown in figure 3.19. From the line of equality of figure 3.18 it is clear that the ultrasonic dynamic modulus is considerably greater than its static counterpart. However the electrodynamic modulus results are comparable to their static modulus values for granite concrete. The same trend is shown in figure 3.19 for andesite concrete, however, neglecting result A for the electrodynamic plots produces a regression line very close to the line of equality showing that for the andesites, the static modulus value is very similar to the corresponding electrodynamic modulus value.

Table 3.10(a) Average Values of Electrodynamic and Ultrasonic Dynamic Modulus for Granite Concrete

STONE CONTENT kg/m^3	CEMENT/ WATER RATIO	ELECTRODYNAMIC MODULUS GPa	ULTRASONIC DYNAMIC MODULUS GPa
700	1,5	34,08	46,89
	1,8	28,38	49,57
	2,4	30,65	52,40
1000	1,5	28,92	50,05
	1,8	35,53	54,17
	2,4	32,79	56,14
1300	1,5	30,44	53,97
	1,8	27,27	56,98
	2,4	35,17	60,04

Table 3.10(b) Average Values of Electrodynamic and Ultrasonic Dynamic Modulus for Andesite Concrete

STONE CONTENT kg/m^3	CEMENT/ WATER RATIO	ELECTRODYNAMIC MODULUS GPa	ULTRASONIC DYNAMIC MODULUS GPa
700	1,5	31,40	55,83
	1,8	22,01	58,50
	2,4	35,26	62,62
1000	1,5	34,07	62,70
	1,8	34,97	65,73
	2,4	39,89	68,75
1300	1,5	36,66	67,59
	1,8	38,54	71,05
	2,4	41,56	74,72

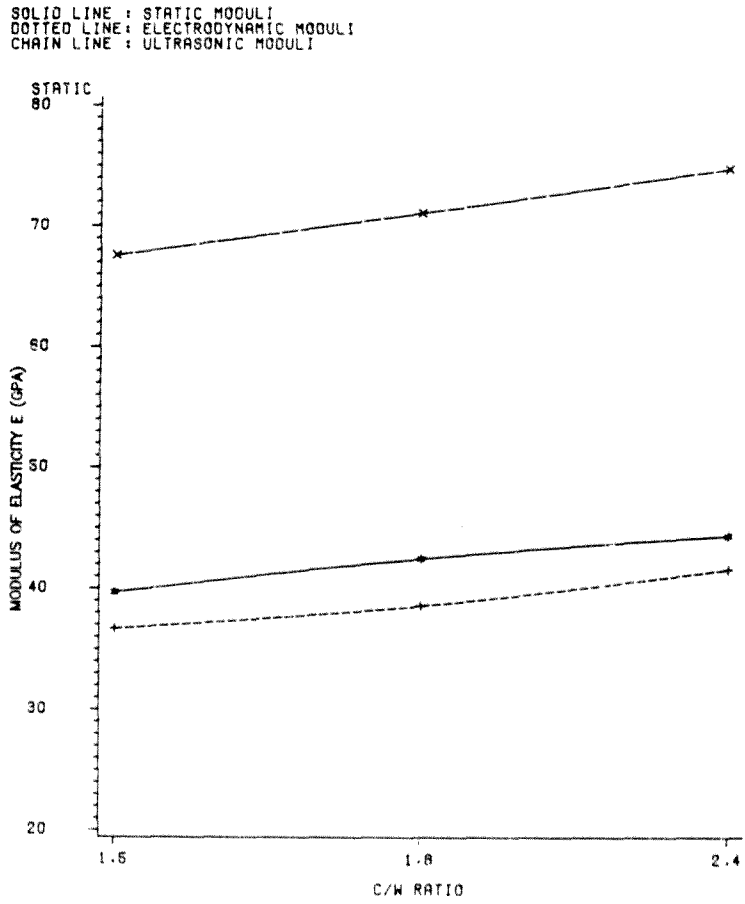

FIG 3.17 C/W RATIO VS. MODULUS OF ELASTICITY STATIC, ELECTRODYNAMIC AND ULTRASONIC PLOTS FOR ANDESITE CONCRETE 1300 KG/CU.M

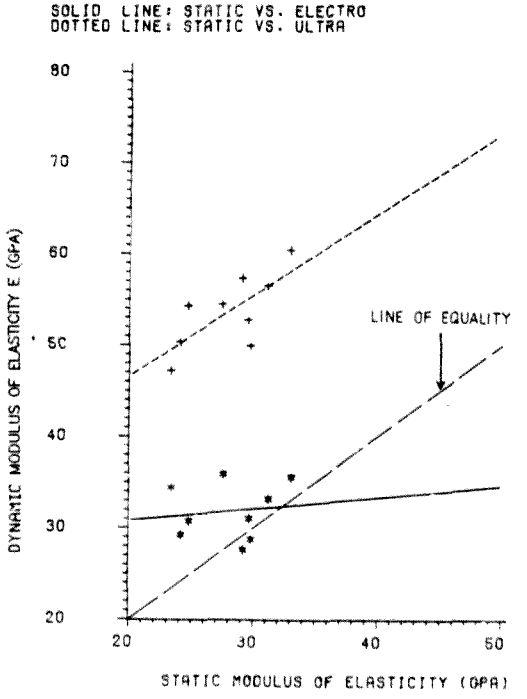

FIG 3.18 STATIC MODULUS VS. ELECTRODYNAMIC MODULUS AND ULTRASONIC MODULUS (GRANITE CONCRETE)

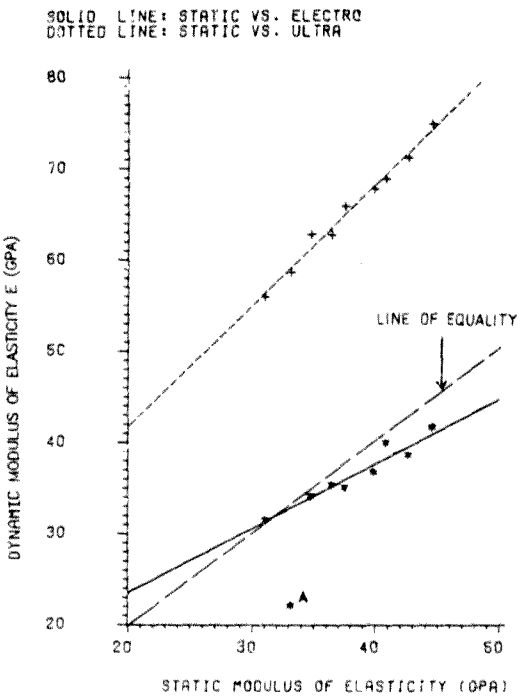

FIG 3.19 STATIC MODULUS VS. ELECTRODYNAMIC MODULUS AND ULTRASONIC MODULUS (ANDESITE CONCRETE)

If a statistically significant number of results were taken, a more accurate relationship could be established between electrodynamic, ultrasonic and static moduli for the two aggregate types. Figure 3.19 shows that the relationship of electrodynamic and ultrasonic moduli to static modulus follows the same form. The plot for static against ultrasonic shows a very definite relationship between the two moduli. If such relationships were established this would facilitate testing procedures. The dynamic tests are much faster and also non-destructive. This would be very beneficial to measure age effects on modulus.

3.10 CONCLUSIONS

1. An increase in stone content leads to an increase in static elastic modulus. The effect is minor for granite concrete but considerable for andesite concrete.

2. Increasing c/w ratio has a marked effect for both aggregate types on static elastic modulus.

3. The andesite mixes gave consistently higher moduli and higher compressive strengths compared to their granite counterparts. For equal compressive strength, andesite aggregate concrete has a higher elastic modulus than granite aggregate concrete, the percentage difference in elastic moduli increasing as the compressive strength of the concrete increases. Values of elastic modulus for granite concrete ranged from 23,5 to 33,2 GPa, 27,3 to 35,5 GPa and 46,9 to 60,0 GPa for static, electrodynamic and ultrasonic moduli respectively; corresponding values for andesite concrete were 30,8 to 44,4 GPa, 22,0 to 41,6 GPa and 55,8 to 74,7 GPa.

4. The stress/strain plots for the concretes were more curved than for the equivalent pastes and mortars. The descending

branch of the complete stress/strain curve after failure was more pronounced and extensive than that of the mortars, due to the composite action of the concrete and its ability to carry reduced stress at higher strain levels.

5. The ultrasonic modulus was considerably higher than its static and electrodynamic counterparts for both aggregate types. The difference was considerably greater for the andesite mix.

6. The prism strength of each mix was considerably lower than the cube strength, probably due to the effects of aspect ratio and the stiffness of the testing machine. The interparticle contact occurring in high stone contents may also have a reducing effect on the compressive strength of the prisms.

CHAPTER 3

REFERENCES

1. TEYCHENNE, W.C., PARROTT, L.J., POMEROY, C.D., The Estimation of the Elastic Modulus of Concrete for the Design of Structures Building Research Establishment CP 23/78 pp 1-12.

2. HANSEN, J.C., Theories of Multipnase Materials applied to Concrete, Cement Mortar and Cement Paste. The Structure of Concrete, Proceedings of an International Conference, London September, 1965, pp 16-23.

3. SOROKA I., Portland Cement Paste and Concrete. MacMillan Press Ltd., 1979, pp 234.

4. ILLSTON, J.M., DINWOODIE, J.M., SMITH, A.A., Concrete Timber and Metals. The Nature and Behaviour of Structural Materials. Von Nostrand Reinhold. International Student Edition, London 1979, pp 273.

5. MAHER, A., DARWIN, D., Mortar constituent of Concrete in Compression. ACI Journal, March-April 1982, pp 100-109.

6. HOBBS, D.W., The Strength and Deformation of Concrete under Short Term Loading: A Review, Cement and Concrete Association. Technical Report No. 42, 484 London 1973, pp 1-10.

7. DAVIS, D.E., THOMPSON, C.W., Movement in Concrete Structures. Concrete Society of Southern Africa, Johannesburg, 1981 pp 8-10.

8. DAVIS, D.E., THOMPSON, C.W., op cit p 11.

9. BEEBY, A.W., Modified Proposals for Controlling Deflections by means of Ratio of Span to Effective Depth. Technical Report 42.456 London, Cement and Concrete Association, 1971 p 19.

10. HOBBS, D.W., Drying Shrinkage and Movement of Reinforced Concrete. Technical Report 42.522 Wexham Springs, Cement and Concrete Association 1978, p 19.

11. ILLSTON, J.M., et al., op cit p 205.

12. SOROKA, I., op cit p 242.

13. REICHARD, J.W., Creep and Drying Shrinkage of Lightweight and Normal Weight Concrete. Monograph No. 74, National Bureau of Standards, Washington 1964.

14. SHIDELER, J.J., Lightweight Aggregate Concrete for Structural Use. Proc. Am. Conc. Institute., 54, No. 9, 1957 pp 299-328.

REFERENCES/cont..

15. SOROKA, I., op cit p 242.

16. SOROKA, I., op cit p 250-257.

17. PARROTT, L.J., Simplified Methods of Predicting the Deformation of Structural Concrete. Technical Report No. 3, Cement and Concrete Association Wexham Springs, 1979 pp 10-11.

18. TEYCHENNE, W.C., et al op cit p 8.

19. SOROKA, I., op cit p 234.

20. MINDESS, S., YOUNG, J.F., Concrete. Prentice Hall Inc. 1981 pp 477-480.

21. FELDMAN, R.F., AND BEAUDOIN, J.J., Microstructure and Strength of Hydrated Cement. Symposium Chem. Cement Moscow 1974.

22. SOROKA, I., op cit p 202.

23. PARROTT, L.J., op cit pp 6-8.

24. MONFORE, G.E., AND LENTZ, A.E., Physical Properties of Concrete at Low Temperatures. Portland Cement Association Journal, Vol 4, No. 2, May 1962 pp 33-9.

25. DAVIS, H.S., Effects of High-Temperature Exposure on Concrete Materials Research and Standards, Vol 7, No. 10, October 1967 pp 452-9.

26. KAPLAN, M.F., Effects of incomplete Consolidation on Compressive and Flexural Strength, Ultrasonic Velocity and Dynamic Modulus of Elasticity of Concrete. American Concrete Institute Journal, Proc. V. 56, No. 9, March 1960 pp 853-868.

27. CP 110 The Structural Use of Concrete, Part 1. British Standards Institution, London 1972.

28. South African Bureau of Standards. The structural use of concrete, SABS 0100, Part 1 - 1980. SABS, Pretoria, 1980.

29. CEB/FIP International Recommendations for the Design and Construction of Concrete Structures. Cement and Concrete Association 1970.

30. ACI Committee 318. Building Code Requirements for Reinforced Concrete. Detroit, American Concrete Institute, 1977, ACI Publication 318-77.

REFERENCES/cont.

31. DAVIS, D.E., The Concrete making Properties of South African Aggregates. PHD Thesis submitted to the University of Witwatersrand, 1974 pp 156-171.

32. ALEXANDER, M.G., AND ABERDEIN, D.A., Elasticity of Plain Concrete and Mortar Specimens in Flexure and Compression. The Civil Engineer in South Africa, Vol 25, No. 4, 1983, pp 205-215.

33. WEIBULL, W., A statistical Theory of the Strength of Materials Proceedings of Royal Swedish Institute for Engineering Research, Stockholm 1939, 151, 5.

34. HOGNESTAD, E., HANSON, N.W., AND McHENRY, D., Concrete Stress Distribution in Ultimate Strength Design. Journal of the American Concrete Institute, Proceedings Vol 52, No. 12 December 1955, pp 455-479.

35. BRITISH STANDARDS INSTITUTION. BS 1881 Part 121, 1983. Method for Determination of Static Modulus of Elasticity in Compression. London pp 1-3.

36. AMERICAN SOCIETY FOR TESTING AND MATERIALS Standard Test Method for Static Modulus of Elasticity and Poisson's Ratio of Concrete in Compression. ASTM C469-81 Philadelphia, 1981 pp 299-303.

37. NEVILLE, A.M., Properties of Concrete. Third Edition, London, Pitman Publishing Limited, 1981 pp 537-545.

38. MINDESS, S., AND YOUNG, J.F., op cit., p 420.

39. KAPLAN, M.F., Ultrasonic Pulse Velocity, Dynamic Modulus of Elasticity, Poisson's Ratio and Strength of Concrete Made with 13 Different Coarse Aggregates. Rilem Bulletin No. 1 March, 1959, pp 58-73.

40. MINDESS, S., AND YOUNG, J.F., op cit., pp 377-378.

41. SOROKA, I., op cit pp 242-243.

CHAPTER 4 THEORETICAL MODELS FOR ESTIMATING ELASTIC MODULUS OF CONCRETE

4.1 INTRODUCTION

Concrete is a multi-phase composite material. At the macroscopic level it consists of particles of coarse aggregate embedded in a mortar matrix, whilst the mortar consists of sand grains in a matrix of cement paste. At the microscopic level, cement paste consists of cement gel with an almost continuous system of water filled or dry capillary pores. At the submicroscopic level, cement gel is basically a mixture of semi-amorphous interwined fibrous particles. Combined with thin crumpled sheets it forms a continuous matrix having a more or less continuous system of minute water-filled voids called gel pores. Embedded in the gel are also unhydrated cement grain cores. Most aggregates are also multi-phase composite materials with a pronounced porosity and consisting of different crystalline or amorphous components[1].

In spite of the complexity of the material structure, mathematical analysis of the influence of concrete composition on the physical behaviour of the material is possible, provided the assumptions are made that certain phases are isotropic, homogeneous and discrete. Concrete may be analysed as a two-phase material consisting of aggregate particles embedded in matrix of mortar, if the aggregate phase and mortar phase are considered to be homogeneous and isotropic. The following equations and mathematical analysis follows the micro-rheological approach described by Hashin[2]. This is in contrast to macro-rheological analysis which is based on the behaviour of models consisting of ideal elastic, plastic and viscous elements which are coupled in series or parallel to behave like real materials when subjected to load or deformation. Similar to elastic analysis, macro-rheology assumes that all materials are isotropic and homogeneous, but like elastic analysis does not explain anything about the physical mechanisms responsible for the mechanical behaviour of materials.

Micro-rheology is based on geometrical models which resemble the real structure of the material as closely as possible. It provides an understanding of the correlation between material structure and mechanical properties and hence is a valuable tool in material science. However, this type of analysis is applicable only when the phases are taken to be continuous media. Elementary micro-rheological principles can lead to approximate methods for estimating mechanical behaviour of concrete from a knowledge of mix proportions and the mechanical properties of the respective components.

In this final chapter, I shall compare the elastic moduli estimated from five representative theoretical equations with actual measured concrete elastic moduli. The equations predict elastic moduli from a knowledge of the mix proportions and mechanical properties of the aggregate, paste and mortar. The object is to gauge which equations render accurate predictions of measured concrete behaviour.

4.2 Factors Affecting Composite Behaviour

Before applying the composite approach to concrete, let us first consider the behaviour of composites in general. In order to describe a system with one or more dispersed phases embedded in a continuous matrix, the following parameters must be considered:

a) shape of particles
b) size and size distribution of particles
c) concentration and concentration distribution of particles
d) orientation of particles
e) composition of the dispersed phase
f) composition of continuous phase
g) bond between the continuous and dispersed phases

As the microstructure of concrete is very complex, a simple description of the geometry of the system in terms of the above would be difficult. Also, it is difficult to determine which phase is continuous or disperse. To simplify matters, let us consider the two extreme cases of phase arrangement; that is the series and parallel systems shown in figure 4.1. These systems are used to calculate the elastic parameters of a composite system if the elastic parameters of the individual phases are known.

It has been suggested by Hansen[3] that a composite material like concrete can have two fundamentally different structures:-

1. Structure of an ideal composite soft material

This has elastic particles with a high modulus of elasticity embedded in a continuous matrix phase with a lower modulus of elasticity.

2. Structure of an ideal composite hard material

This has a continuous lattice of an elastic phase with a high modulus of elasticity, with embedded particles having a lower modulus of elasticity.

In the following analysis the symbols used are:

ϵ_c = strain in concrete
ϵ_a = strain in aggregate
ϵ_m = strain in matrix
σ = stress in concrete
σ_a = stress in aggregate
σ_m = stress in matrix
E_c = elastic modulus of concrete
E_a = elastic modulus of the aggregate
E_m = elastic modulus of the matrix
g = volume concentration of the aggregate

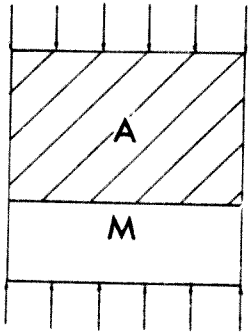

(a)

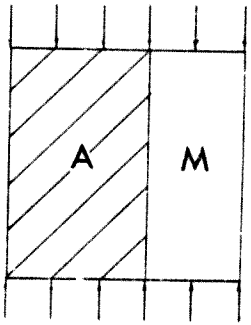

(b)

where A = aggregate
M = matrix

Figure 4.1 Models of the structure of concrete

(a) series (constant stress) model
(b) parallel (constant strain) model
(after Mindess[4])

A series model can be used to calculate the modulus of elasticity of a composite soft material. The assumption is that the stress over any section of the material is the same, while the strains are additive. Using strain compatibility the strain in the concrete, ε_c, is, for unit area:-

$$\varepsilon_c \cdot 1 = \varepsilon_a \cdot g + \varepsilon_m(1-g) \qquad \ldots\ldots (4.1)$$

Since $\varepsilon_c = \frac{\sigma}{E_c}$, $\frac{\sigma_a}{E_a} = \varepsilon_a$, $\sigma_p = \frac{\varepsilon}{E_p}$ $\qquad \ldots\ldots (4.2)$

We have,

$$\frac{\sigma}{E_c} \cdot 1 = g \cdot \frac{\sigma_a}{E_a} + (1-g)\frac{\sigma_p}{E_p} \qquad \ldots\ldots (4.3)$$

But $\sigma = \sigma_a = \sigma_m$

Therefore

$$\frac{1}{E_c} = \frac{g}{E_a} + \frac{(1-g)}{E_m} \qquad \ldots\ldots (4.4)$$

or expressed in general terms for a two phase model

$$E_c = \frac{1}{g/E_a + (1-g)/E_m} \qquad \ldots\ldots (4.5)$$

The series system in which the phases are subjected to uniform stresses provides the lower bound solution. It is sometimes refe-red to as the Ruess model.

The modulus of a composite hard material may be calculated on the assumption that the strain is the same over any section of the material whilst the stresses in the phases are proportional to the modulus of elasticity of the phases. The parallel system, in which the two phases are subjected to uniform strains, provides the upper bound solution for the elastic parameter of interest. Considering the parallel model using strain compatibility, the strain in the concrete, ε_c is equal to the strain in the aggregate, ε_a and the hardened cement paste (h.c.p.), ε_m ie

$$\varepsilon_c = \varepsilon_a = \varepsilon_m \qquad \ldots\ldots (4.6)$$

For equilibrium the total force applied to the model is given by the applied stress, σ acting on unit area. Thus

$$\sigma.1 = \sigma_a.g + \sigma_m(1 - g) \qquad \ldots\ldots (4.7)$$

Both constituent materials are assumed elastic as is the concrete, therefore

$$\sigma = \varepsilon_c E_c; \quad \sigma_a = \varepsilon_a E_a; \quad \sigma_m = \varepsilon_m E_m \qquad \ldots\ldots (4.8)$$

Substituting in equation 4.7 from equation 4.8 and then using equation 4.6 :-

$$E_c = E_a g + E_m (1-g) \qquad \ldots\ldots (4.9)$$

The parallel model is sometimes referred to as the Voigt model.

Hansen[3] found that equation 4.5 gives a better approximation of the elastic modulus when the aggregate is stiffer than the matrix (ie $E_a > E_p$), which is generally the case in concrete. Equation 4.9 is more suited for conditions where the aggregate is softer than the matrix material (ie $E_a < E_p$). In fact neither model is absolutely correct, since concrete under load exhibits neither uniform stress nor uniform strain within the phases. For concretes made with natural aggregates, Mindess and Young[4] state that the series model underestimates E_c by about ten per cent, while the parallel model overestimates E_c by a greater amount.

Other models have been proposed to predict concrete behaviour. Hirsch[5] suggested a model which is the geometric sum of equation 4.5 and 4.9, given in equation 4.10:

$$\frac{1}{E_c} = (x)\left[\frac{1}{(1-g)\,E_m + gE_a}\right] + (1-x)\left[\frac{(1-g)}{E_m} + \frac{g}{E_a}\right] \qquad \ldots\ldots (4.10)$$

where x and (1-x) are the relative proportions of material conforming with the upper and lower bound solutions. It has been

found for some concretes that x is approximately 0,5[5]. Note that when there is no bond between the matrix and the aggregate (x=0) equation 4.10 reduces to equation 4.5 (the uniform stress model). For perfect bond (x=1) equation 4.10 reduces to equation 4.9 (the uniform strain model). Although Hirsch's model produces good results over a wide range of variables, (average deviation ± 10% and a maximum deviation ± 35%)[5] it has one limitation: for $E_a = 0$ equation 4.10 (and equation 4.5) predict $E_c = 0$ which is clearly erroneous. It predicts the modulus of elasticity of porous solids, irrespective of pore content, to be zero. Hirsch's model is shown diagramatically in figure 4.2(a).

Another physical model propored by Counto[6] is shown in figure 4.2(b). Counto's model can be expressed as

$$\frac{1}{E_c} = \frac{1 - g^{1/2}}{E_m} + \frac{1}{[(1-g^{1/2})/g^{1/2}]\,E_m + E_a} \qquad \ldots\ldots (4.11)$$

This is intuitively more satisfactory in that it actually bears some resemblance to concrete. Counto found that estimates made with this model agree fairly well with experimental data. He carried out a comparative study of the above four models for the prediction of the elastic modulus of concrete, using worldwide data from various laboratories covering an unusually wide variety of aggregate and concrete mixes. The study showed that Counto's model gave the best overall approximation with an average deviation of + 7,83% and - 8,86%[6]. However in many cases there is little variation between estimates of Hirsch's model and those of Counto[7].

A realistic model for concrete has been proposed by Hobbs[8]. The model is based on a phase arrangement of spherical aggregate particles embedded in a continuous matrix. Hobbs's model can be expressed by:-

$$E_c = \left[\frac{(E_a-E_m)g + (E_m+E_a)}{(E_a+E_m) + (E_m-E_a)g}\right] E_m \qquad \ldots\ldots (4.12)$$

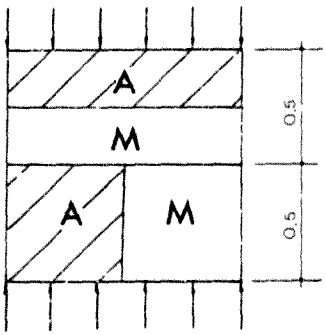

(a)

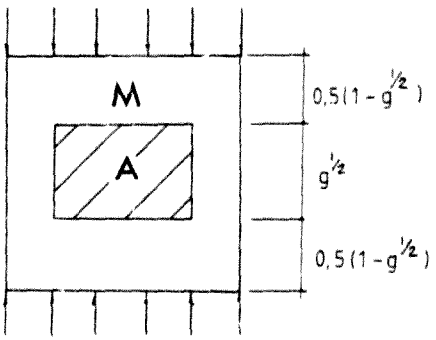

(b)

where A = aggregate
M = matrix

Figure 4.2 Models of the Structure of Concrete
(a) Hirsch's model[5] (b) Counto's model[6]

The equation is strictly valid when :-

1) there is no interaction between adjacent aggregate particles and

2) there is perfect bond between the aggregate and the matrix

The first assumption is reasonable, but the second assumption is not totally valid, and extensive bond failure occurs at stresses higher than about 40 per cent of concrete strength. The degree of bond failure between aggregate and matrix will govern the validity of application of the model to real concrete[9]. In fact, Hobbs's model is identical to Hansen's[1] model given in equation 4.13 below, which is a rearrangement of equation 4.12. Hansen's model can be written as :-

$$E_c = E_m \left[\frac{(1-g)E_m + (1+g)E_a}{(1+g)E_m + (1-g)E_a}\right] \qquad \ldots\ldots (4.13)$$

Hansen's and Hobbs's model is shown in figure 4.3(a). The aggregate phase is represented by a sphere at the centre of a sphere of concrete. The fractional volume of the aggregate is the same as the fractional volume of aggregate particles in concrete. The equation giving the bulk modulus for the model was developed by Hashin[10]. Hansen utilised Hashin's equation, and assuming Poisson's ratio of the paste, aggregate and concrete were equal to 0,2 he derived equation 4.13. Theoretically, Poisson's ratio may vary from -1,0 to +0,5 hence this could be a source of error in the equation. Practically, Poisson's ratio for saturated concrete lies in the range +0,2 to +0,3, but decreases on drying to fall in the range 0,15 to 0,20, with a mean value of about 0,18[11]. The dynamic Poisson's ratio is slightly higher, averaging about 0,24 and this is probably more representative of elastic behaviour[11]. The validity of equation 4.13 is also subject to the two main assumptions made for equation 4.12.

Further models have been proposed by Paul[12] and Ishai[13]. Paul's model is shown in figure 4.3(b) and represents the aggregate as a cube which is placed at the centre of a concrete cube. Paul's model differs from Counto's in that Counto's model postulates a cylinder (or prism) of aggregate located centrally in a cylinder (or prism) of concrete. Both cylinders (or prisms) have the same ratio of height to area of cross section. Paul's model is one of a cubic aggregate within a cubic matrix subject to a uniform normal stress at the boundary. Counto's model assumes uniform stress distribution which is incompatible with the physical boundary conditions in axial loading of a heterogeneous material. Assuming uniform boundary stress, the modulus of elasticity for Paul's model is given by :-

$$E_c = E_m \left[\frac{1 + (E_a/E_m - 1) g^{2/3}}{1 + (E_a/E_m - 1)(g^{2/3} - g)} \right] \qquad \ldots\ldots (4.14)$$

Ishai[13] extended Paul's work and showed that the modulus of elasticity of concrete assuming a uniform boundary strain rather than stress was :-

$$E_c = E_m \left[\frac{g}{(E_a/E_m)/(E_a/E_m - 1) - g^{1/3}} + 1 \right] \qquad \ldots\ldots (4.15)$$

Ishai's model was found to give better agreement with experimental results than Counto's when epoxy resin composites containing a high concentration of quartz sand were compared[13].

Teychenne et al[14] used Hobbs's equation to calculate moduli for a composite (concrete) from a range of typical values of E_p (modulus of the paste), E_a and g. These values are tabulated in table 4.1. It is apparent that the influence of the aggregate volume concentration when E_a has a lower value is comparatively small and the effects of the paste and aggregate moduli predominate. However, for aggregates with high moduli the effect of aggregate volume concentration can have a significant effect. The table also shows that the modulus of the aggregate has a considerable effect on the modulus of the concrete.

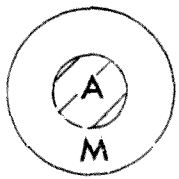

(a)

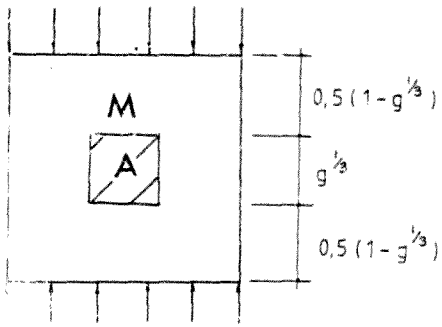

(b)

where A = aggregate
M = matrix

Figure 4.3 Models of the Structure of Concrete
(a) Hansen's model[1]
(b) Paul's model[12]

Table 4.1 Elastic Moduli of Concrete Composite Calculated using Hobbs Equation (after Teychenne et al[14])

Aggregate Volume Concentratio (V_a)	Elastic Modulus (kN/mm^2)			
	Cement Paste E_m	Aggregate E_a		
		20	60	100
0,65	5	11	18	19
	10	15	27	32
	15	18	34	43
	20	20	39	51
0,70	5	12	20	22
	10	16	30	37
	1	18	37	47
	20	20	42	55
0,75	5	13	22	26
	10	17	32	42
	15	18	40	52
	20	20	44	60
0,80	5	14	26	31
	10	17	37	48
	15	19	43	58
	20	20	47	66

It is a matter of debate as to which of the aforementioned equations is basically more correct with respect to the actual behaviour of concrete. It can be seen from figure 4.4 that quantitatively, with the exception of the series and parallel models, the other three models lie fairly close to one another. This is despite the fact that they are all based on different assumptions. It may be concluded that the aggregate affects the modulus of elasticity of concrete, primarily by virtue of its stiffness and secondarily by its concentration. In general, the modulus of elasticity of concrete increases with increase in modulus of aggregate. In normal concrete, for which $E_a > E_p$, the modulus of the concrete also increases with increase in concentration of aggregate. Conversely, in lightweight aggregate concrete, for which $E_a < E_p$, the modulus decreases with increasing concentration of aggregate[15]. However, as stated above, the effects of aggregate concentration are less significant than the modulus of the aggregate itself.

4.3 Comparison of Theoretical Models with Measured Values for Elastic Modulus of Concrete

In comparing the various theoretical models, the following points must be borne in mind. The aggregates used in the tests are not ideal spherical shapes and do not act completely independently of each other. As shown in chapter 3 inter-particle contact is evident at the upper stone content of 1300 kg/m^3 and to a lesser extent at 1000 kg/m^3. Although the andesite aggregate is a comparatively 'stiff' aggregate, it is not inordinately stiffer than the 'softer' granite aggregate. Although the granite concrete is not as stiff as the andesite concrete it could not be strictly classed as a concrete made with a soft aggregate. Differences between the two concretes might be expected, but these differences would not be as striking as would occur if very low modulus aggregate (for example a weathered granite) had been used.

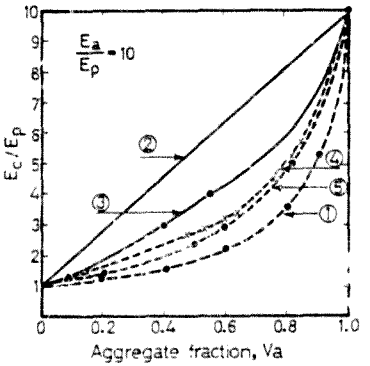

Figure 4.4 Effect of Aggregate Concentration on Modulus of Elasticity (after Kameswara et al[6])

1) Series model (equation 4.5)
2) Parallel model (equation 4.9)
3) Hirsch's model (equation 4.10)
4) Counto's model (equation 4.11)
5) Hobbs's model (equation 4.12)

As stated and commented on in chapter 2, the results for pastes and granite mortars with cement/water ratios of 1,5 and 1,8 must be viewed with caution. The measured elastic moduli in these cases was somewhat lower than expected. The measured prism strengths were also below the expected values. It is thought that some different kind of material behaviour may have been taking place. Although the prism strengths measured in chapter 3 for the concrete mixes were also much lower than the cube strengths (all expected strengths being based on that of concrete cube strength) there was no apparent adverse effect on the measured moduli. Hence it was thought inadvisable to use the 'unrepresentative' modulus values for the abovementioned pastes and mortars in the model calculations. Therefore, only representative calculations and curves were tabulated and plotted.

From the mix design parameters in chapter 3, the various volume fractions of the components were calculated. Using different components of the concrete as the matrix phase (eg the paste or mortar phases) values of elastic modulus were calculated using the equations given above. Thus a comparison could be made between the theoretical estimated value derived from the equations and the actual measured elastic modulus for that concrete mix. Various combinations were calculated, namely :-

a) coarse and fine aggregate in a paste matrix
b) coarse aggregate in a mortar matrix
c) the paste modulus was used to predict the mortar modulus, which in turn was used to predict the concrete elastic modulus.

A family of curves was plotted for each of the cases given above, and for each of the theoretical models (with the exception of the parallel model which gave exceptionally high values for elastic modulus), according to the format given in figure 4.5 below:-

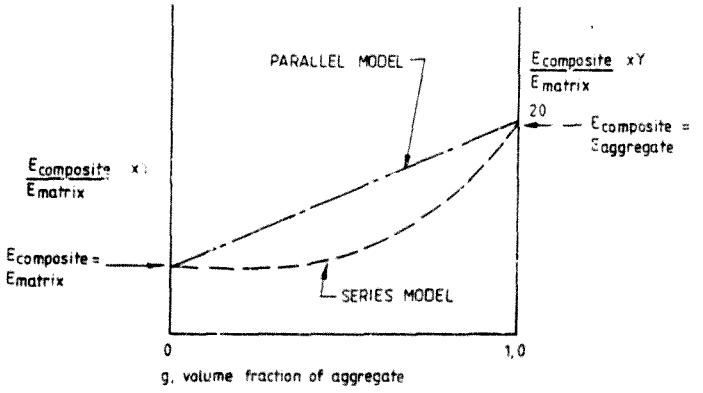

Figure 4.5 The Effect of Aggregate Concentration on Modulus of Elasticity of Concrete

The plots do not show the effect of aggregate on an individual model, but comparison of models. The plots are derived in the following manner. For each theoretical model the measured E of the concrete is divided by the measured E of the matrix and th s in turn is multiplied by a factor Y:-

$$\frac{\text{measured } E_{composite}}{\text{measured } E_{matrix}} \times Y$$

Where Y is a factor $= \frac{E_{matrix}}{E_{aggregate}} \times 20$ (say)

The number 20 is just an arbitrary numerical value which all the model curves are constrained to pass through at g = 1. Clearly when g = 1,0 we have $E_{composite} = E_{aggregate}$.

Therefore at g = 1,0

$$\frac{\text{measured } E_{composite}}{\text{measured } E_{matrix}} \times \frac{E_{matrix}}{E_{aggregate}} \times 20$$

$$= \frac{E_{composite}}{E_{aggregate}} \times 20$$

$$= 20$$

Therefore all the theoretical model curves were constrained to pass through the [illegible] means of this factoring. This was done in order [illegible] compare the prediction effectiveness of the composite mo[illegible]ing the matrix and volume fractions; the closer each theoretical plot to the experimental plot, the more accurate the model.

4.3.1 Coarse and Fine Aggregate in a Paste Matrix

Table 4.2(a) shows the results for granite concretes. The Series model (equation 4.5) predicts the elastic modulus with remarkable accuracy giving an overall percentage difference of approximately 5%. The Parallel model grossly overpredicts the measured moduli. This was consistently the case throughout the theoretical model calculations. Therefore the Parallel model was omitted from the plots. Hobbs's model also overpredicts the measured moduli (by an average of 20%) as does Hirsch's and Counto's models. This is clearly seen from figure 4.6(a) with the Series model clearly the nearest plot to the experimentally derived plot of measured values.

* Series Model + Hirsch's Model x Counto's Model
□ Hobbs's Model △ Experimental Results

E_k = Calculated or measured elastic modulus
c/w = Cement/water ratio
Y = 20

Table 4.2(a) Comparison of Measured Elastic Moduli of Concrete with those Predicted by Theoretical Equations (Coarse and Fine Aggregate in a Paste Matrix for Granite Concrete, E_a = 81,30 GPa)

C/W Ratio	Stone Content kg/m³	E_{Paste} GPa	Volume Fraction of Aggregate (Coarse + Fine) g	$E_{Concrete}$ Predicted by Equation:- GPa 4.5	4.9	4.10	4.11	4.12	Measured $E_{Concrete}$ GPa
2,4	700	13,93	0,588	27,19	53,71	36,10	35,22	33,81	29,78
	1 000		0,647	30,06	57,70	39,52	38,74	37,50	31,37
	1 300		0,709	33,81	61,89	43,73	43,07	42,03	33,24
		Average % Difference		4,87	83,50	20,25	23,78	19,85	

$$\% \text{ DIFFERENCE} = \frac{E_{(measured)} - E_{(predicted)}}{E_{(measured)}} \times 100$$

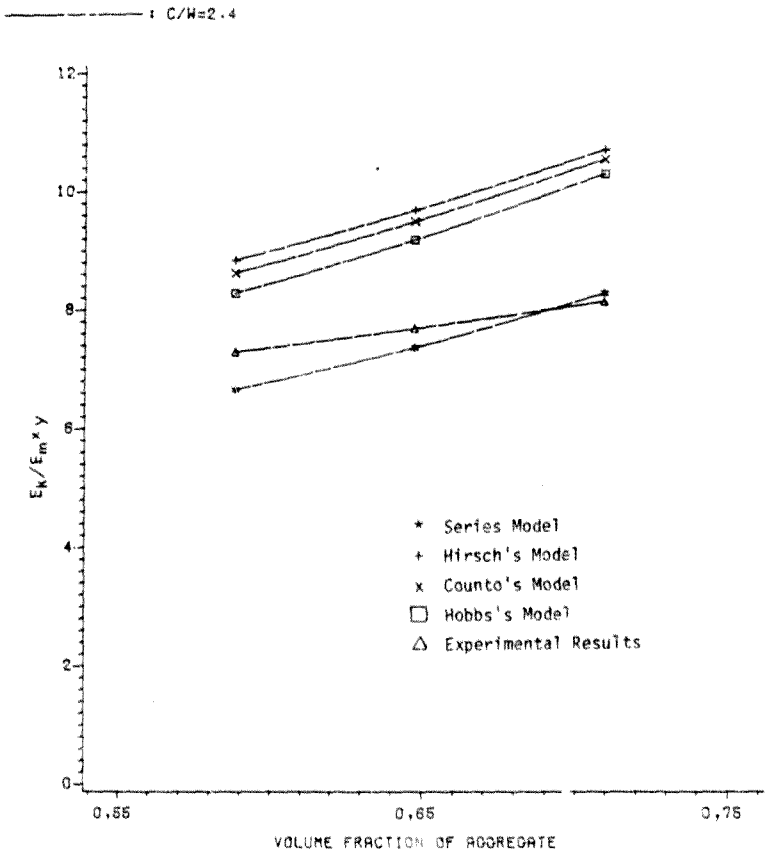

FIG 4.6a COARSE AND FINE AGGREGATE IN A PASTE MATRIX THEORETICAL MODEL PREDICTIONS AND MEASURED VALUES FOR GRANITE CONCRETE

The values for andesite concrete are given in table 4.2(b) and plotted in figure 4.6(b). In this case Hobbs's model predicts the elastic modulus to less than 3% percentage average difference. For the two lower stone contents, the model predicts the value with remarkable accuracy. Again, Hirsch's and Counto's models overpredict the modulus by up to 10% average difference. The Series model underpredicts the moduli in this instance on average by approximately 20%. For a normal concrete with E aggregate > E matrix, the Series model would be expected to underestimate the actual concrete moduli. This is true for the andesite concretes but only partially true for the granite concrete. For this particular combination it seems that the Series model renders accurate predictions for the granite concretes and Hobbs's model gives the best predictions for the andesites.

4.3.2 Coarse Aggregate in a Mortar Matrix

Table 4.3(a) gives the results for granite concrete and figure 4.7(a) shows the plots of the models and the measured elastic modulus values. In this case all the models overestimate the measured elastic moduli. Again, the Series model renders the closest prediction to the actual results. The Hirsch, Counto and Hobbs models yield very similar results, all overestimating the value in excess of 30%. For the granite mortar with cement/water ratio 2,4 the measured elastic modulus is identical to the measured elastic modulus value for the concrete of 700 kg/m^3 stone content, which is somewhat in contrast with model predictions.

Table 4.3(b) and figure 4.7(b) (c) and (d) shows the results and plots for the andesite concrete respectively. In this case all three cement/water ratios were calculated. Consistently throughout all cement/water ratios the Series model predicts the measured values with remarkable accuracy, especially at the

Table 4.2(b) Comparison of Measured Elastic Moduli of Concrete with those Predicted by Theoretical Equations (Coarse and Fine Aggregate in a Paste Matrix for Andesite Concrete, E_a = 104,40 GPa)

C/W Ratio	Stone Content kg/m^3	E_{Paste} GPa	Volume Fraction of Aggregate (Coarse + Fine) g	$E_{Concrete}$ Predicted by Equation:- GPa 4.5	4.9	4.10	4.11	4.12	Measured $E_{Concrete}$ GPa
2,4	700	13,93	0,588	28,40	67,13	39,92	38,54	36,68	36,21
	1 000		0,647	31,71	72,46	44,11	42,88	41,20	40,60
	1 300		0,709	36,13	78,07	49,40	48,34	46,91	44,35
		Average % Difference		20,67	79,97	10,09	7,02	2,85	

$$\% \text{ DIFFERENCE} = \frac{E_{(measured)} - E_{(predicted)}}{E_{(measured)}} \times 100$$

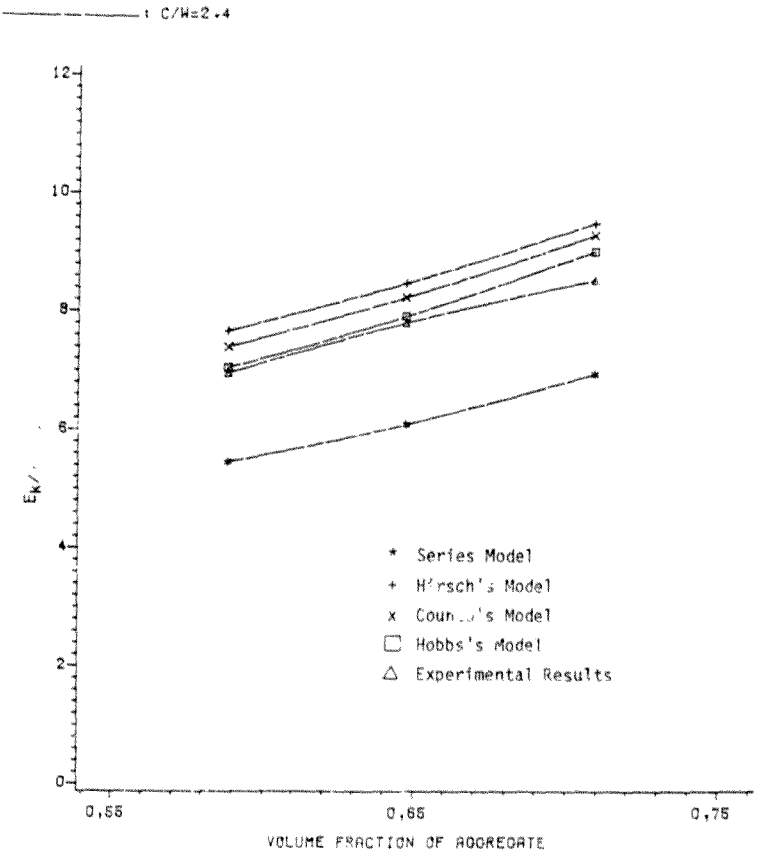

FIG 486 COARSE AND FINE AGGREGATE IN A PASTE MATRIX
THEORETICAL MODEL PREDICTIONS AND MEASURED
VALUES FOR ANDESITE CONCRETE

Table 4.3(a) Comparison of Measured Elastic Moduli of Concrete with those Predicted by Theoretical Equations (Coarse Aggregate in a Mortar Matrix for Granite Concrete, E_a = 81,30 GPa)

C/W Ratio	Stone Content kg/m^3	E_{Mortar} GPa	Volume Fraction of Aggregate (Coarse) g	$E_{Concrete}$ Predicted by Equation - GPa 4.5	4.9	4.10	4.11	4.12	Measured $E_{Concrete}$ GPa
2,4	700	29,78	0,254	35,51	42,94	38,87	38,95	37,76	29,78
	1 000		0,364	38,73	48,64	43,12	43,09	41,92	31,37
	1 300		0,473	42,56	54,28	47,71	47,62	46,58	33,24
		Average % Difference		24,23	54,96	37,89	37,85	34,21	

$$\% \text{ DIFFERENCE} = \frac{E_{(measured)} - E_{(predicted)}}{E_{(measured)}} \times 100$$

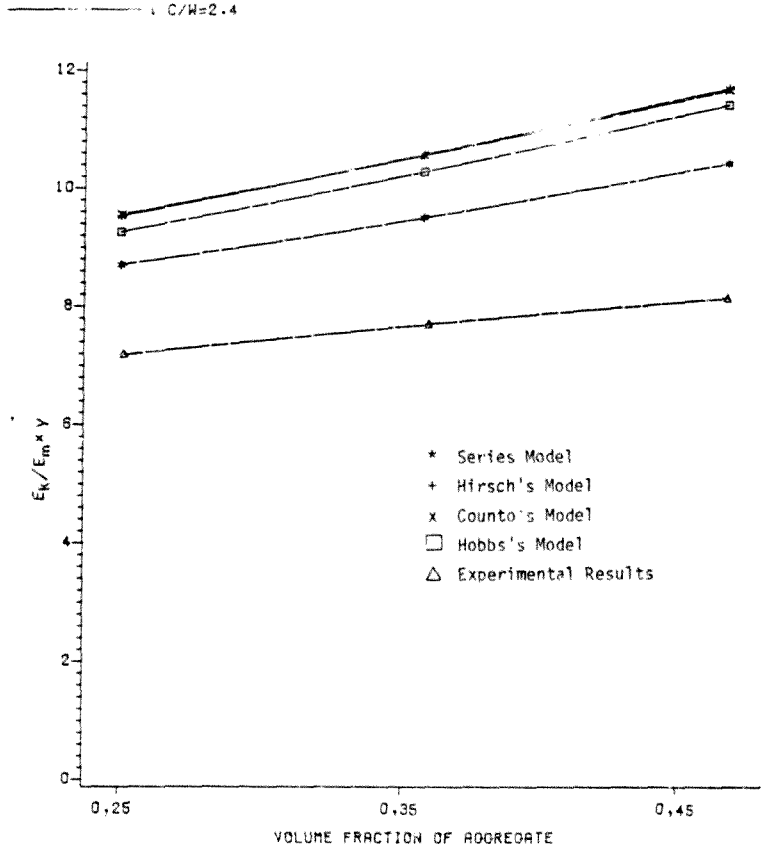

FIG 4.7a COARSE AGGREGATE IN A MORTAR MATRIX THEORETICAL MODEL PREDICTIONS AND MEASURED VALUES FOR GRANITE CONCRETE

Table 4.3(b) Comparison of Measured Elastic Moduli of Concrete with those Predicted by Theoretical Equations (Coarse Aggregate in a Mortar Matrix for Andesite Concrete, E_a = 104,40 GPa)

C/W Ratio	Stone Content	E_{Mortar}	Volume Fraction of Aggregate (Coarse)	$E_{Concrete}$	Predicted by Equation:- GPa				Measured $E_{Concrete}$
	kg/m^3	GPa	g	4.5	4.9	4.10	4.11	4.12	GPa
1,5	700	24,61	0,254	30,54	44,88	36,34	35,80	33,78	30,81
	1000		0,364	34,10	53,65	41,69	40,96	38,91	34,50
	1300		0,473	38,54	62,35	47,64	46,86	44,96	39,66
		Average % Difference		1,62	52,80	19,64	17,70	11,93	
1,8	700	25,39	0,254	31,43	45,46	37,17	36,68	34,68	32,93
	1000		0,364	35,04	54,15	42,55	41,87	39,85	37,34
	1300		0,473	39,55	62,76	48,52	47,79	45,92	42,43
		Average % Difference		7,46	96,46	33,37	29,75	18,69	
2,4	700	26,70	0,254	32,92	46,44	38,53	38,12	36,16	36,21
	1 000		0,364	36,62	54,98	43,96	43,37	41,39	40,60
	1 300		0,473	41,21	63,45	49,96	49,32	47,50	44,35
		Average % Difference		8,66	35,58	9,12	7,77	3,06	

$$\% \text{ DIFFERENCE} = \frac{E_{(measured)} - E_{(predicted)}}{E_{(measured)}} \times 100$$

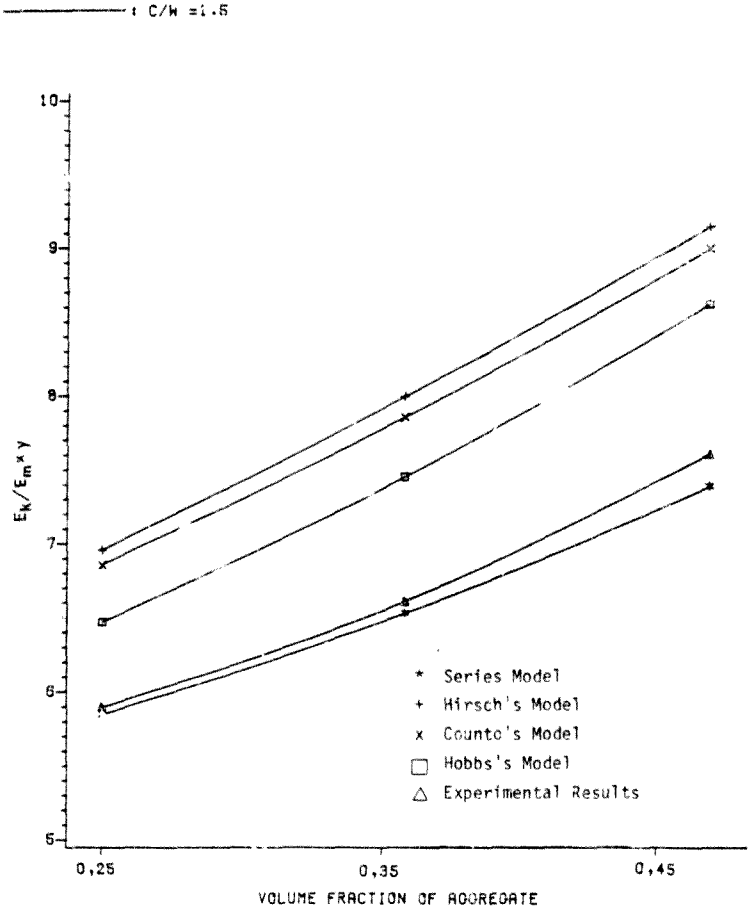

FIG 4.7b COARSE AGGREGATE IN A MORTAR MATRIX
THEORETICAL MODEL PREDICTIONS AND MEASURED
VALUES FOR ANDESITE CONCRETE

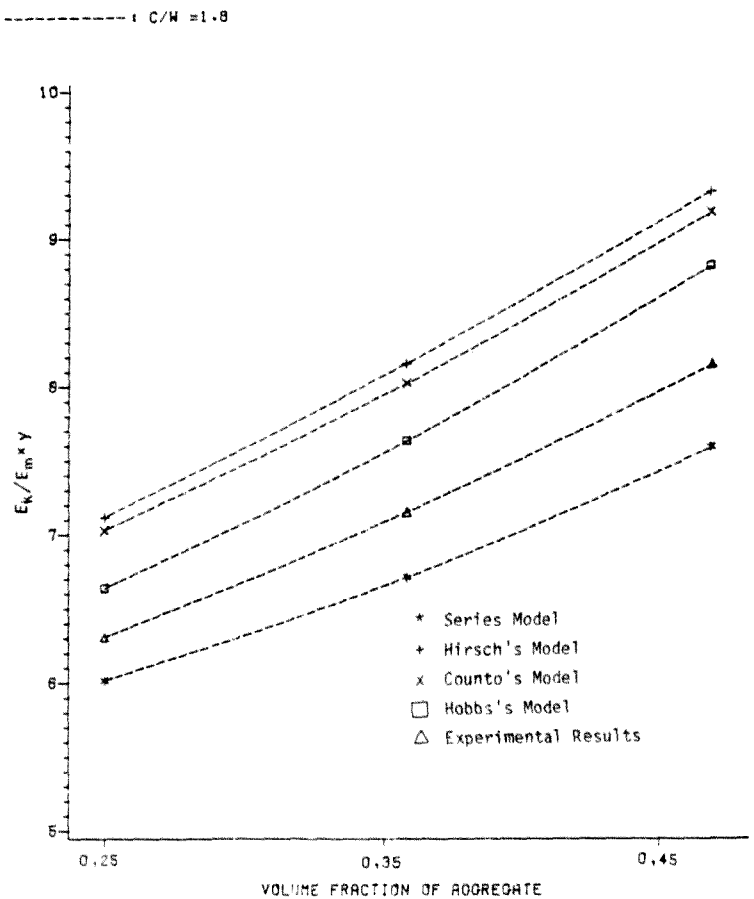

FIG 4.7c COARSE AGGREGATE IN A MORTAR MATRIX THEORETICAL MODEL PREDICTIONS AND MEASURED VALUES FOR ANDESITE CONCRETE

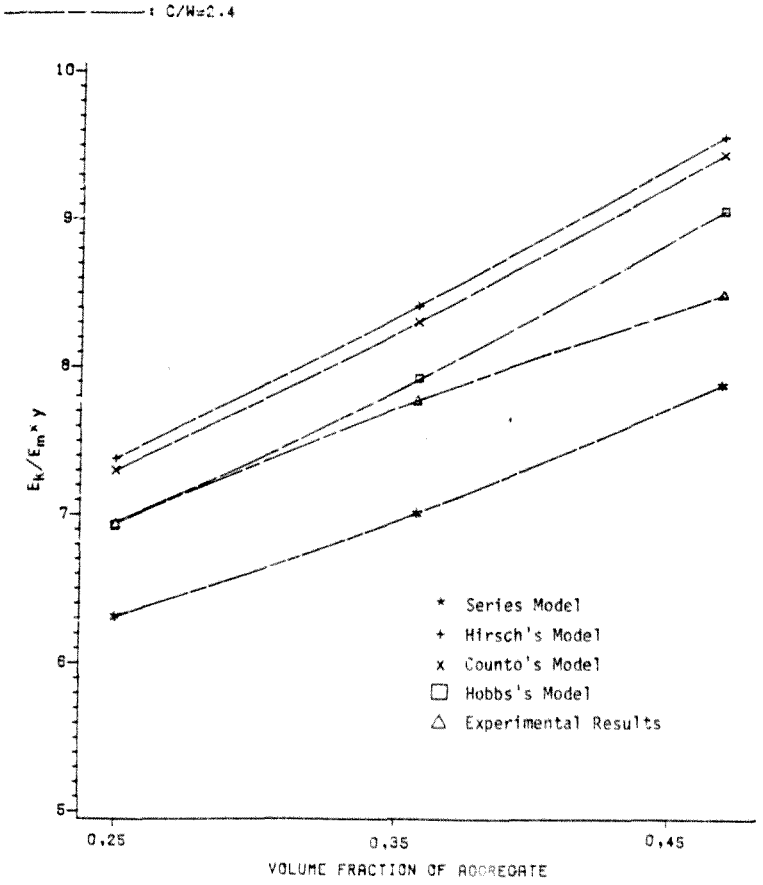

FIG 4.7d COARSE AGGREGATE IN A MORTAR MATRIX
THEORETICAL MODEL PREDICTIONS AND MEASURED
VALUES FOR ANDESITE CONCRETE

lowest cement/water ratio. The average percentage difference between the measured and predicted results is 6%. In general, this is an underestimate of the measured elastic moduli. Hobbs's equation renders a more accurate prediction at the high cement/water ratio than the Series model, but on average only predicts with a percentage difference of approximately 11%. Hirsch's and Counto's models render very similar results, as evidenced by plots.

For this permutation, the Series model renders the best overall prediction for both granite and andesite concretes; however, for a high cement/water ratio, the Hobbs model renders the closest prediction.

4.3.3 Paste Modulus used to Predict Mortar Modulus, the resulting Modulus being used to Predict the Final Concrete Modulus

The results and plots for granite and andesite concretes are shown in table 4.4(a) and (b) and figure 4.8(a) and (b) respectively. For the granite concrete the Series model again predicts the most accurate value for cement/water ratio of 2,4. the percentage difference being approximately 5%. Excluding the parallel model, the other models overpredict the elastic modulus by between 25% and 35%. Counto's equation predicts the elastic modulus of the granite mortar to less than 1% difference and Hirsch's equation to less than 5%. Even though the Series model only predicts the elastic modulus of the granite mortars to 25% of the measured value, the model still renders the most accurate prediction of measured values for concrete. The Series model's final prediction is a slight underestimate of the measured values. Figure 4.8(a) shows the comparison of the models for granite concrete.

Table 4.4(a) Comparison of Elastic Modulus of the Paste used to Predict Elastic Modulus of Mortar then finally the Modulus of the Granite Concrete, E_a = 81,30 GPa)

C/W Ratio	Stone Content kg/m³	E of Cement Paste GPa	Volume Fraction of Sand in Cement Mortar	E of Mortar Predicted by Equation GPa 4.5	4.9	4.10	4.11	4.12	Measured E of Mortar GPa	Volume Fraction of Stone in Concrete	E of Concrete Predicted by Equation GPa 4.5	4.9	4.10	4.11	4.12	Measured E of Concrete GPa
	700									0,254	27,16	53,67	38,60	37,70	34,74	29,78
2,4	1 000	13,93		,13	44,17	29,49	28,50	26,84	29,78	0,364	30,12	57,79	42,86	41,86	38,93	31,37
	1 300									0,473	33,77	61,86	47,46	46,43	43,68	33,24
	Average % Difference			25,67	48,32	0,97	4,31	9,88			4,80	83,52	36,33	33,25	24,05	

$$\% \text{ DIFFERENCE} = \frac{E_{(measured)} - E_{(predicted)}}{E_{(measured)}} \times 100$$

Table 4.4(b) Comparison of Elastic Modulus of the Paste used to Predict Elastic Modulus of Mortar then finally the Modulus of the Andesite Concrete, E_a = 104,40 GPa)

C/W Ratio	Stone Content kg/m³	E of Cement Paste GPa	Volume Fraction of Sand in Cement Mortar	E of Mortar Predicted by Equation GPa 4.5	4.9	4.10	4.11	4.12	Measured E of Mortar GPa	Volume Fraction of Stone in Concrete	E of Concrete Predicted by Equation GPa 4.5	4.9	4.10	4.11	4.12	Measured E of Concrete GPa
	700									0,254	28,38	67,08	43,94	42,20	38,05	36,21
2,4	1 000	13,93	0,447	22,74	54,37	32,07	30,51	28,39	26,70	0,364	31,79	72,58	49,45	47,54	43,33	40,60
	1 300									0,473	36,09	78,03	55,48	53,50	49,47	44,35
	Average % Difference			14,84	33,63	20,10	14,27	6,35			20,65	79,99	22,75	18,09	7,79	

$$\% \text{ DIFFERENCE} = \frac{E_{(measured)} - E_{(predicted)}}{E_{(measured)}} \times 100$$

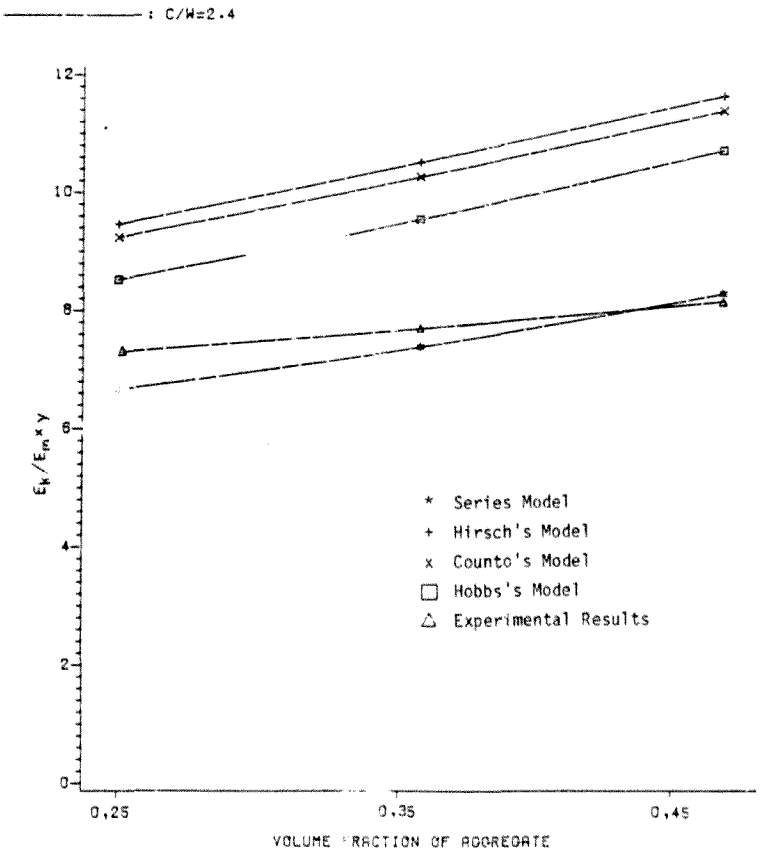

FIG 4.8a PASTE MODULUS USED TO PREDICT THE MORTAR MODULUS, RESULTING MORTAR MODULUS TO PREDICT CONCRETE MODULUS (GRANITE CONCRETE)

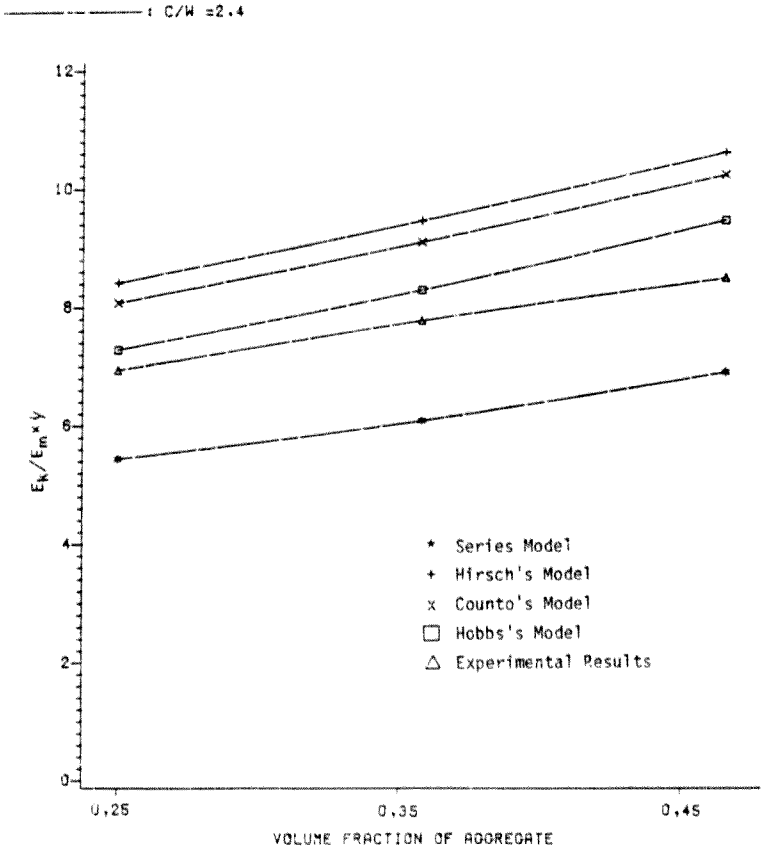

FIG 4.8b PASTE MODULUS USED TO PREDICT THE MORTAR MODULUS, RESULTING MORTAR MODULUS TO PREDICT CONCRETE MODULUS (ANDESITE CONCRETE)

Hobbs's model gives the most accurate values for the andesite concretes. It predicts the modulus to better than 10 percent accuracy. The Hobbs model also predicted the andesite mortar with the most accuracy. The Series model, and Hirsch's and Counto's model predicted values of approximately 20 percent above the measured values. For this combination the Series model gave the most consistent results for the granite concretes and the Hobbs model for the andesites.

4.4 Comparison of Back-Calculated Theoretical Values of Elastic Moduli for Pastes and Mortars with Unrepresentative Values

For the cement/water ratios 1,5 and 1,8 for pastes and granite mortars (for which the results were deemed unrepresentative), theoretical values of E_m were back-calculated. The back-calculated values would give some indication of the influence of voids and other phenomena which could have affected the experimental results. For each combination, eg. coarse and fine aggregate particles in a paste matrix, the theoretical equation which gave the closest approximation to the experimentally determined value of elastic modulus for cement/water ratio 2,4 in that particular combination was utilised to back-calculate E values from representative concrete elastic modulus values for cement/water ratios of 1,5 and 1.8. The results of these calculations are given in tables 4.5 and 4.6 for the pastes and granite mortars respectively. The granite concretes were back-calculated using the Series model and the andesites using the Hobbs model.

Clearly the experimentally determined paste elastic modulus values are gross underestimates of the back-calculated values as table 4.5 indicates. The measured values are approximately half those of the theoretical back-calculated values. This seems

Table 4.5 Comparison of Back-Calculated Theoretical Values of E_p and Experimental Values

Type of Concrete	Cement/ Water Ratio	Back-Calculated E_p GPa	Experimental E_p GPa	% Difference
Granite	1,5	8,95	4,55	+ 96,7
	1,8	12,[illegible]	5,87	+104,6
Andesite	1,5	8,75	4,55	+ 92,3
	1,8	10,47	5,87	+ 78,4

Table 4.6 Comparison of Back-Calculated Theoretical Values of E_{mortar} and Experimental Values, Granite Mortar

Type of Concrete	Cement/ Water Ratio	Back-Calculated E_m GPa	Experimental E_m GPa	% Difference
Granite	1,5	17,16	14,38	+ 19,3
	1,8	20,70	20,14	+ 2,8

to indicate that many voids were present leading to unrepresentative values of elastic modulus for the paste. This also could explain the lower compressive strengths as compressive strength is even more sensitive to the presence of voids than is elastic modulus. An interesting point is the close parity of the back-calculated values for the paste of cement/water ratio 1,5, bearing in mind that they were back-calculated by two different theoretical equations.

However, the experimental results of the granite mortars are not inordinately different from the back-calculated values. This is particularly the case for the granite mortar cement/water ratio 1,8 as table 4.6 shows. Therefore this value may not be 'unrepresentative' due to the small percentage difference between the theoretical back-calculated value and the measured value. As stated in chapter 2, the mortars were much more robust and not as many voids were in evidence, as was the case with the pastes. Therefore, even though the granite mortars gave lower E values than their andesite counterparts, at least the value for cement/water ratio of 1,8 could have been included as a representative value for the granite mortar. However, since the back-calculations are taken from so few results and are only an indication, it was decided to disregard the experimentally determined values of cement/water ratio 1,5 and 1,8 for the granite mortars.

4.5 Discussion on Theoretical Models

Almost without exception for all the combinations examined, the Series model renders the most accurate predictions for the granite concretes and the Hobbs model is the most accurate for the andesite concretes. It also seems from the results that the best prediction combination for both concretes is coarse and fine aggregate in a paste matrix. In this prediction combination

using the results for 2,4 c/w ratio concrete, the granite concrete elastic modulus was calculated to only 4,9 percentage difference using the series model. The andesite concrete elastic modulus was predicted to a 2,9 percentage difference of the experimentally determined value. However, with the exception of the granite concrete calculated using coarse aggregate in a mortar matrix (the Series model only predicting the elastic modulus to a 24,2 percentage difference), the other equations predict the measured values to within 10 percent. However, I feel that it is more accurate to use a combination involving only one calculation to arrive at the theoretical value of E_c, eg. coarse and fine aggregate in a paste matrix, or coarse aggregate in a mortar matrix. The reason for this is that all the models have a number of simplifying assumptions. The models are approximate and therefore calculations involving the models should be simple to perform for practical purposes. Table 4.4 (a) shows that for granite concrete where E_{paste} was used to predict E_{mortar}, which in turn was used to predict $E_{concrete}$, the Series model (omitting the Parallel model) renders the most inaccurate value for E_{mortar}. However, when the E_c is estimated from this value, it renders the closest approximation to the measured concrete moduli. This is an apparent inconsistency.

In retrospect, the laboratory work and in particular the paste work, showed that the most practical and accurate prediction combination is coarse aggregate in a mortar matrix, utilising the Series model for granite concretes and the Hobbs model for the andesites. The laboratory work demonstrated the difficulty in accurately assessing E values for pastes, particularly at low cement/water ratios; therefore E_c predictions from these values would have to be viewed with caution due to possible voids in the pastes used for the matrix elastic modulus values.

4.6 Conclusions

(a) From the results deemed to be representative, the Series model is the most accurate for the various prediction combinations examined for granite concretes. The Hobbs model is the most accurate model for the various prediction combinations for andesite concretes.

(b) Coarse aggregate in a mortar matrix is the most practical and simplest prediction combination for both types of concrete reviewed in this dissertation.

(c) The Hirsch and Counto models rend[illegible]r results to those of the Hobbs model. Howeve[illegible]er is more consistently accurate in its predic[illegible]ffectiveness. The Parallel model greatly overestimates the elastic modulus for both concrete types. The Series model in general slightly underestimates the measured elastic moduli.

(d) Provided accurate estimates of low cement/water ratio pastes could be obtained, the elastic modulus of concrete could be accurately predicted employing a suitable theoretical model.

(e) The results show that inconsistencies occur in the ability of the various models to predict moduli. For example, the Series model predicted a very good concrete modulus for the granite concrete, but a rather poor modulus for the granite mortar. These inconsistencies are bound to arise due to the simplifying assumptions inherent in the models, and their inability to account for physical factors such as particle shape.